JOURNAL OF CHEMICAL & ENGINEERING DATA

ARTICLE

pubs.acs.org/jced

$p-\rho-T$ Behavior of Three Lean Synthetic Natural Gas Mixtures Using a Magnetic Suspension Densimeter and Isochoric Apparatus from (250 to 450) K with Pressures up to 150 MPa: Part II

M. Atilhan,[*,†] S. Aparicio,[‡] S. Ejaz,[§] D. Cristancho,[∥] I. Mantilla,[§] and K. R. Hall[§]

[†]Chemical Engineering Department, Qatar University, Qatar

[‡]Chemistry Department, University of Burgos, Spain

[§]Artie McFerrin Department of Chemical Engineering, Texas A&M University, College Station, Texas, United States

[∥]Molecular Structure/Thermal Department, The Dow Chemical Company Midland OPS, Michigan, United States

Supporting Information

ABSTRACT: Work reported in this paper is the continuation of a previous work (Atilhan et al. *J. Chem. Eng. Data* **2011**, *56*, 212−221) and reports measurements of density and phase envelope characteristics of three synthetic natural gas-like mixtures. These mixtures consist of primarily 0.9000 methane in mole fraction and variable amounts of ethane, propane, 2-methylpropane, butane, 2-methylbutane, and pentane as well as the presence or absence of nitrogen and carbon dioxide. A high-pressure single-sinker magnetic suspension densimeter was used to measure the density of the mixtures along three isotherms at (250, 350, and 450) K with pressures up to 150 MPa. Density measurements are compared to the GERG04 and AGA-8 equations of state, which are the two leading models used for natural gas density predictions. Predictions from both equations have a similar agreement with the data, yet it is observed that GERG04 model shows better performance in predictions with deviations less than around 0.2 % at different temperatures (T = 350 K and T = 450 K) and pressures (p > 20 MPa). An isochoric apparatus was used for phase envelope experiments, and the data are compared to several cubic biparametric, cubic triparametric, and molecular-based equation of states. Equation-of-state predictions for the mixtures and comparison with the experimental data are shown. Equation-of-state predictions show substantial deviations around the entire phase envelope for the third mixture, in which the nitrogen and carbon dioxide have not been included.

1. INTRODUCTION

This project is a combined effort between Qatar University, Texas A&M University, and The National Institute of Standards and Technology (NIST); the densities of the same mixtures are also measured in NIST laboratories via a two-sinker magnetic suspension densimeter, and these data were recently published in this journal.[2]

Knowledge of the pressure−density−temperature ($p-\rho-T$) behavior of natural gas at reservoir and pipeline conditions has been an interest of academia since the beginning of the second quarter of the last century, and it is extremely necessary for several practical applications. Most importantly, custody transfer metering of natural gas has great commercial importance, which requires very accurate density data.[3] Simple models predict densities of natural gas in the custody transfer region within a ± 1 % relative deviation with respect to reliable experimental data, which is not sufficient for custody transfer.[4,5] The gas industry uses cubic equations of state (EOS's) to predict phase envelopes since ease of use and wide availability in commercial packages provide quick solutions, and they do not require high computational requirements.[6] However, although these models are useful for some applications, the uncertainty of their predictions requires oversizing many industrial designs. Molecular-based EOS's have stronger theoretical foundations than cubic equations; however, practical use of these EOS is limited by their complexity and slow computational speed.[7]

Besides, as a requirement for accurate density data, accurate knowledge of the phase equilibrium behavior of natural gas is essential for industrial applications such as storage, processing, and transportation through pipelines as contractual disputes between the supplier and purchaser are settled based on the accurate density data.[8]

This paper aims to provide accurate data on density and phase envelope behavior for three synthetic natural gas (SNG) mixtures; thus, these data can be used in EOS development. The density data presented here were measured by using a high-pressure single sinker magnetic suspension densimeter. Moreover, the same SNG gas samples were shipped to NIST, and they were measured via a low pressure two-sinker magnetic suspension densimeter, and these data have been recently published by McLinden.[2] The most important aspect of the density data presented here is that these data were measured at extremely high pressures, which compliment the high accuracy data that was taken by McLinden. Density data are compared with the two most common and comprehensive models that are used for

Received: May 5, 2011
Accepted: August 18, 2011
Published: August 29, 2011

Table 1. Mixture Compositions in Mole Fraction

component	SNG-2	SNG-3	SNG-4
methane	0.89990	0.89975	0.90001
ethane	0.03150	0.02855	0.04565
propane	0.01583	0.01427	0.02243
2-methylpropane	0.00781	0.00709	0.01140
butane	0.00790	0.00722	0.01151
2-methylbutane	0.00150	0.00450	0.00450
pentane	0.00150	0.00450	0.00450
nitrogen	0.01699	0.01713	
carbon dioxide	0.01707	0.01699	

natural gas density predictions, namely, the GERG04[9] EOS and AGA-8[10] EOS.

Experimental phase envelope data are compared with predictions from several widely used cubic equations with bi- and triparametric versions and molecular based EOS's. The Peng–Robinson (PR),[11] Soave–Redlich–Kwong (SRK),[12] Twu–Redlich–Kwong (TRK),[13] Patel–Teja (PT),[14] Mohsin-Nia–Modarress–Mansoori (MMM),[15] statistical associating fluid theory (SAFT),[16] and perturbed-chain (PC)-SAFT[17] equations are compared to the data.

2. EXPERIMENTAL SECTION

2.1. Samples. Three synthetic natural gas samples were prepared gravimetrically by Accurate Gas Products, LLC in Lafayette, LA. The samples that are used in this work are named SNG-2, SNG-3, and SNG-4. Measurements on the sample named SNG-1 were published previously.[1] The mixture compositions are given in Table 1.

2.2. Densimeter. A high-pressure single sinker magnetic suspension densimeter was used for the density measurements; the details of this equipment and the schematics were previously described by Atilhan et al.[1,18] This apparatus uses the principles of hydrostatic buoyancy force technique based upon Archimedes' Principle. The details of the application of this principle in densimeter are described by Wagner and Kleinrahm.[19]

The weight of the submerged sinker is measured, and the density of the fluid is:

$$\rho = \frac{m_v - m_a}{V_s(T,P)} \quad (1)$$

In eq 2, m_v is the mass of the sinker in vacuum, m_a is the apparent mass of the sinker in the fluid, and V_s is the calibrated volume of the sinker, which is a function of temperature and pressure. To operate the balance at a nearly constant loading point to improve the accuracy of the measurement, two external compensation weights made from titanium and tantalum are used; therefore eq 1 is modified to incorporate the used external weights as:

$$\rho_{fluid} = \frac{m_s + (m_{Ta} - m_{Ti}) - (W_1 - W_2) - \rho_{air}(V_{Ta} - V_{Ti})}{V_s(T,P)} \quad (2)$$

where W represents the "balance readings" for the "sinker $- W_1$" and "tare $- W_2$" (or zero point) weighings, and note that there is an extra term accounting for the buoyancy effect of the compensation weights in air; however, usually $V_{Ta} \approx V_{Ti}$, and the last term in the numerator is negligible.

Ta and Ti are the external tantalum and titanium weights.

Table 2. Experimental Density Data and Relative Deviations with Respect to the GERG04 and AGA8 Equations for the SNG-2 Mixture

T	p	ρ		
K	MPa	kg·m^{-3}	Δ_{GERG04}	Δ_{AGA8}
250.020	20.023	270.886	0.0576	−0.538
250.028	29.950	314.558	0.1712	−0.362
250.026	49.915	359.992	0.1898	−0.138
250.003	75.019	393.058	0.0936	−0.046
250.032	100.046	416.584	0.1573	0.140
250.038	125.013	434.094	0.0054	0.079
250.068	149.917	449.647	0.1351	0.278
350.002	9.941	69.358	−0.2344	−0.292
349.999	29.912	198.375	0.0027	−0.068
349.997	49.954	268.390	0.0447	−0.078
349.983	74.917	317.783	0.0388	−0.068
350.009	99.972	350.354	0.0211	−0.067
349.996	125.109	374.884	0.0412	−0.039
349.990	149.891	394.219	0.0405	−0.036
350.029	155.022	397.788	0.0447	−0.033
450.038	9.966	49.749	−0.4158	−0.452
450.045	29.976	141.437	−0.0443	−0.080
450.043	49.975	206.865	0.0459	0.027
450.059	68.914	249.744	0.0297	−0.030
450.054	86.155	279.125	0.0413	−0.034
450.027	114.952	315.989	0.0282	−0.035
450.013	137.492	338.320	0.0294	−0.021

2.3. Isochoric Apparatus. A thermostatted high-pressure cell was used as an isochoric (or isomolar) cell for phase envelope measurements.[7] The technique for determining phase envelopes utilized the change of the slope of an isochore as it crossed the phase boundary.[20] The natural gas sample was compressed and charged into the high-pressure cell, and the temperature of the cell was kept constant. Once the pressure and thermal equilibrium were reached, the temperature of the cell was gradually decreased by steps, and at each temperature change, the temperature and the pressure of the system were recorded after allowing enough time to reach equilibrium. These measurements are repeated several times, and later the data are plotted. A technique developed by Acosta-Perez et al. was used to calculate the point where the isochoric line slope changes, which in fact represents the phase envelope point.[21] The details of the application of this method are described in previous work.[1] The details of the apparatus and schematics are given in previous publications.[1,7]

3. RESULTS

Tables 2, 3, and 4 present the experimental density data for SNG-2, SNG-3, and SNG-4, respectively. Similar measurements on the sample named SNG-1 were published previously.[1] For each sample, isotherms at (250, 350, and 450) K were

dx.doi.org/10.1021/je200438t |J. Chem. Eng. Data 2011, 56, 3766–3774

Table 3. Experimental Density Data and Relative Deviations with Respect to the GERG04 and AGA8 Equations for the SNG-3 Mixture

T	p	ρ		
K	MPa	kg·m^{-3}	Δ_{GERG04}	Δ_{AGA8}
250.016	13.964	221.001	−0.302	−1.246
249.977	16.015	243.888	−0.013	−0.995
250.039	17.997	260.725	0.209	−0.797
250.060	20.044	274.663	0.341	−0.675
250.010	22.012	285.917	0.431	−0.589
250.043	24.019	295.545	0.478	−0.530
250.048	26.039	304.022	0.510	−0.487
250.033	27.998	311.340	0.526	−0.451
250.027	30.064	318.245	0.535	−0.421
249.954	14.972	232.693	−0.358	−1.322
249.955	29.966	317.501	0.367	−0.588
250.024	49.999	362.745	0.458	−0.265
250.025	68.966	388.959	0.431	−0.129
249.946	99.877	418.939	0.438	0.057
250.011	149.957	452.141	0.429	0.224
349.973	9.947	70.314	−0.240	−0.301
349.982	11.980	85.763	−0.179	−0.252
349.977	13.975	100.887	−0.112	−0.191
349.984	15.980	115.755	−0.082	−0.185
349.988	17.987	130.202	−0.029	−0.144
349.970	19.973	143.863	0.002	−0.123
349.976	21.985	156.940	0.025	−0.108
349.970	23.988	169.138	0.028	−0.119
349.981	25.975	180.228	−0.079	−0.245
349.976	27.967	191.240	0.168	−0.021
349.986	29.925	200.884	0.157	−0.053
349.950	9.988	70.602	−0.281	−0.342
349.980	29.997	201.665	0.371	0.161
350.011	49.989	272.162	0.696	0.336
349.977	68.881	310.868	0.429	0.044
349.977	99.889	353.595	0.536	0.146
350.015	149.888	397.800	0.617	0.229
450.004	9.978	50.549	−0.075	−0.111
450.011	11.975	60.650	−0.064	−0.107
449.999	13.975	70.681	−0.031	−0.081
450.006	15.980	80.599	0.011	−0.047
450.011	15.981	80.598	0.005	−0.052
450.007	17.996	90.377	0.035	−0.030
449.972	19.972	99.746	0.045	−0.028
449.972	19.971	99.747	0.051	−0.022
449.967	19.971	99.756	0.058	−0.015
449.962	21.980	109.036	0.070	−0.004
449.978	21.982	109.037	0.071	−0.012
450.022	23.988	118.021	0.086	0.001
449.965	25.971	126.646	0.084	−0.003
449.972	27.979	135.059	0.088	−0.008
449.976	29.997	143.225	0.094	0.003
449.992	10.004	50.627	−0.185	−0.221
449.989	29.976	143.108	0.076	−0.015
449.998	49.978	208.936	0.195	0.041
450.029	68.937	252.029	0.230	−0.012
449.994	99.959	300.555	0.255	−0.052
449.995	149.926	351.272	0.272	−0.042

Table 4. Experimental Density Data and Relative Deviations with Respect to the GERG04 and AGA8 Equations for the SNG-4 Mixture

T	p	ρ		
K	MPa	kg·m^{-3}	Δ_{GERG04}	Δ_{AGA8}
249.983	20.028	282.336	0.169	−0.879
249.987	30.030	321.375	0.376	−0.537
249.997	49.946	362.707	0.426	−0.185
249.977	74.931	393.689	0.408	0.045
249.999	100.291	415.832	0.384	0.184
249.918	124.967	432.286	0.238	0.152
249.988	149.990	446.528	0.224	0.224
350.026	9.998	72.258	−0.463	−0.520
350.019	29.984	204.942	−0.101	−0.262
350.013	49.890	272.578	0.117	−0.162
349.993	74.991	320.091	0.157	−0.128
350.000	99.925	351.066	0.159	−0.112
350.018	124.942	374.231	0.131	−0.128
349.944	149.787	393.033	0.182	−0.070
450.043	9.999	51.020	−0.768	−0.799
450.050	30.001	144.981	−0.247	−0.288
450.057	49.945	210.468	0.023	−0.063
450.062	68.926	252.902	0.147	−0.019
450.027	99.965	300.112	0.198	−0.006
450.084	124.928	327.346	0.216	0.014
450.051	149.926	349.140	0.218	0.020

Table 5. Experimental Phase Envelope Points for SNG-2, SNG-3, and SNG-4 Mixtures

SNG-2		SNG-3		SNG-4	
T/K	p/MPa	T/K	p/MPa	T/K	p/MPa
224.81	7.51179	239.31	9.68088	265.60	11.76229
234.14	7.84067	246.53	9.96381	272.00	11.31499
240.85	7.77762	255.80	10.03886	277.61	9.94697
247.15	7.16079	264.02	9.15598	281.37	8.60669
252.47	6.15873	268.88	7.95887	283.76	6.98957
255.15	4.83229	272.04	6.56836	284.14	5.38415
252.44	3.05327	273.15	4.95806	282.33	3.48815
245.28	1.57178	270.60	3.30320	274.23	1.59253

measured. Table 5 presents the experimental phase envelope points for the measured natural gas samples. For each natural gas sample, eight isochores were studied, and for each isochore about 20 pressure and temperature points were collected. In total, for the three samples a total of 480 $p-\rho-T$ points were measured, and all of these isochoric experiment data are presented in the Supporting Information.

Table 6. AAD % Values for SNG-2, SNG-3, and SNG-4 Samples with Respect to AGA8 and GERG04 Equations

	SNG-2			SNG-3			SNG-4		
	250 K	350 K	450 K	250 K	350 K	450 K	250 K	350 K	450 K
GERG04	0.114	0.059	0.090	0.405	0.242	0.113	0.316	0.185	0.259
AGA8	0.226	0.085	0.097	0.571	0.171	0.035	0.317	0.198	0.173

The calibration of the densimeter was done against pure components of methane,[22] ethane,[23] nitrogen,[24] and carbon dioxide[25] in previous works by the authors, and detailed comparisons of the pure component data against reference equations were made in those publications. For all of the measured pure components, an experimental uncertainty of $\pm 3.5 \cdot 10^{-3}$ kg·m^{-3} in density is achieved for pressures greater than 7 MPa, and an experimental uncertainty of $\pm 4.5 \cdot 10^{-3}$ kg·m^{-3} in density is achieved for pressures between (5 and 7) MPa. The densimeter yields data with less than 0.03 % relative deviation in density over the pressure range of (10 to 200) MPa for nitrogen and carbon dioxide with respect to reference

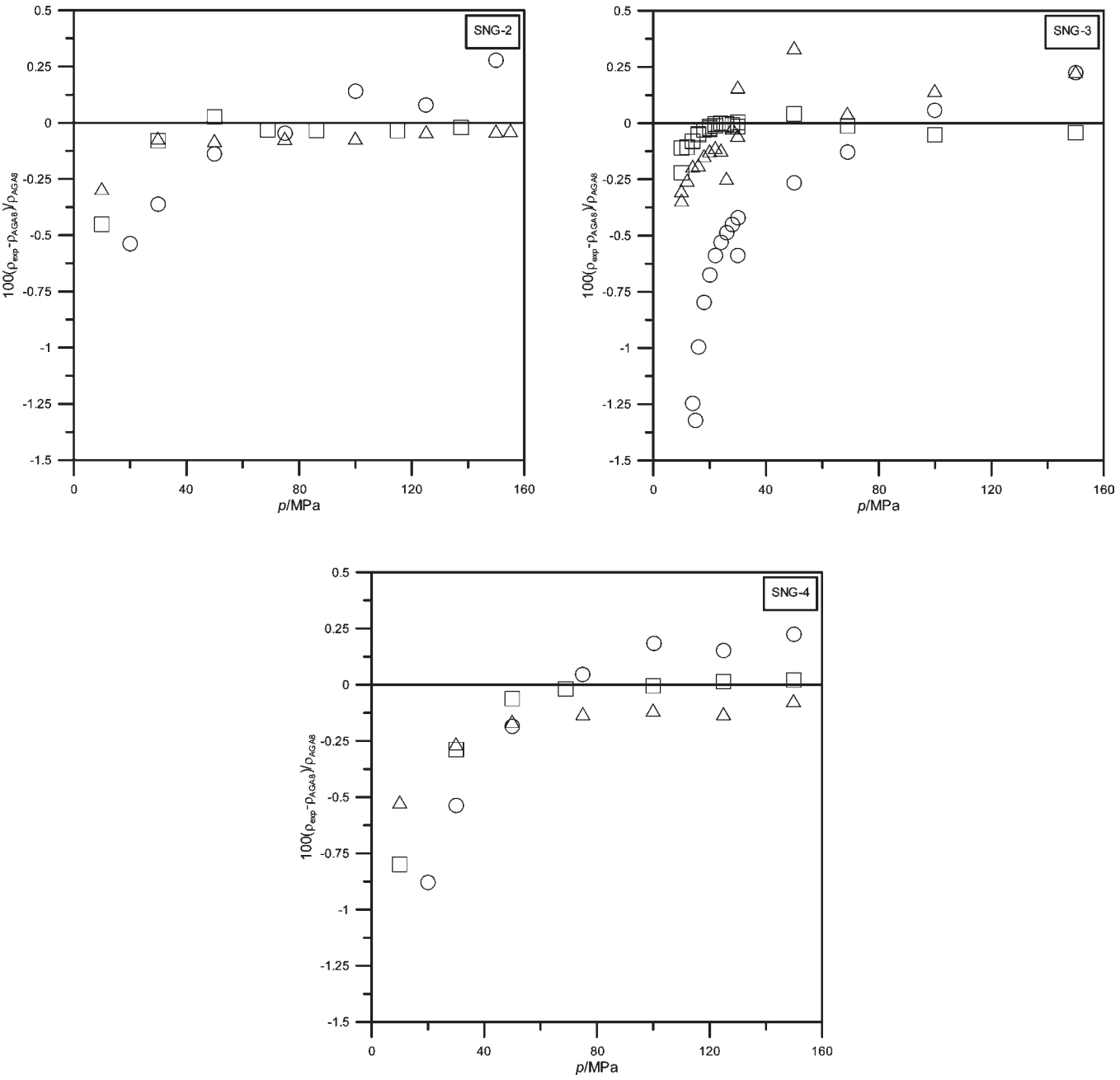

Figure 1. SNG2, SNG3, and SNG4 experimental density deviations with respect to the AGA8 EOS (○, 250 K; △, 350 K; □, 450 K).

dx.doi.org/10.1021/je200438t |J. Chem. Eng. Data 2011, 56, 3766–3774

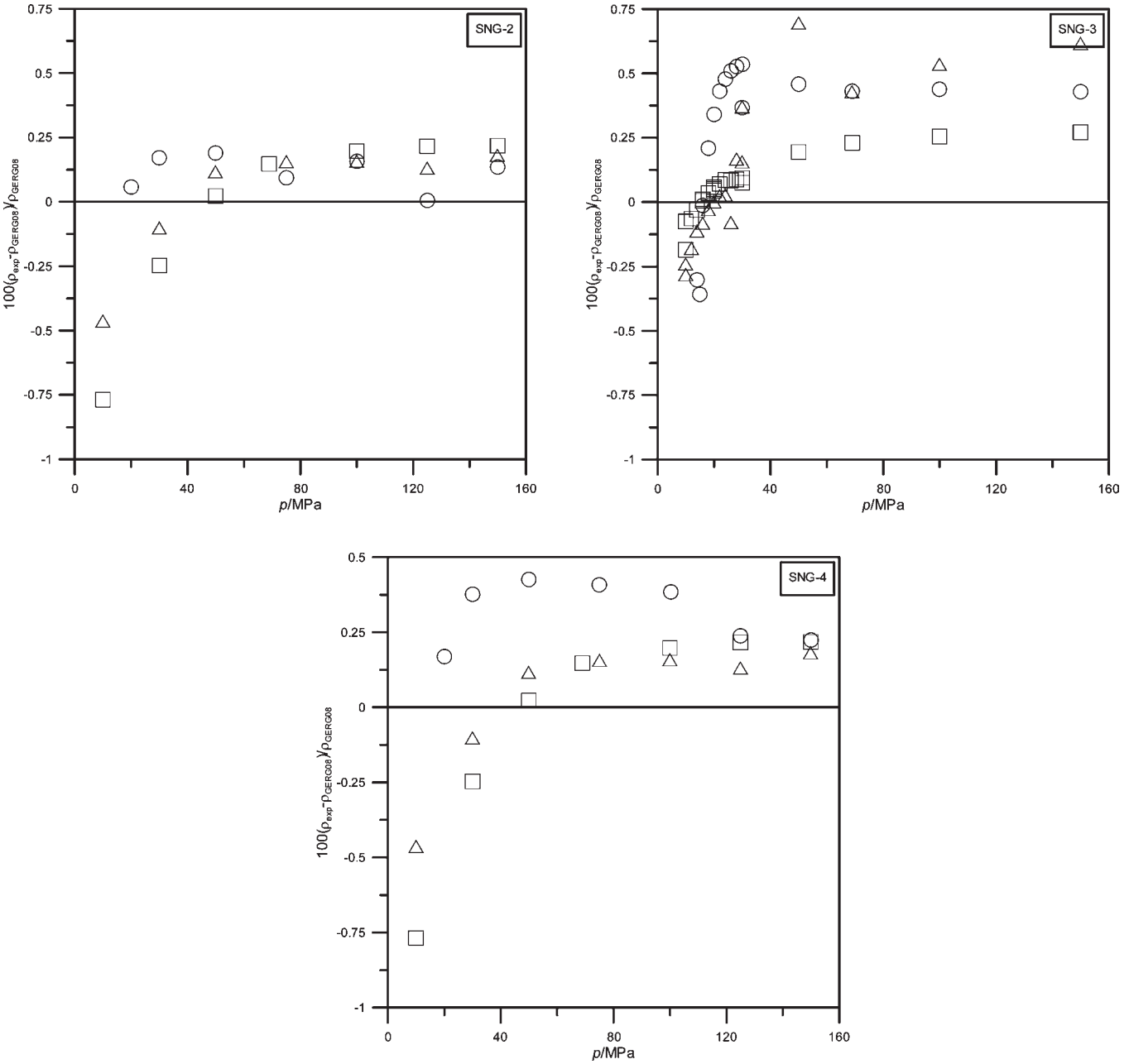

Figure 2. SNG-2, SNG-3, and SNG-4 experimental density deviations with respect to the GERG04 EOS (○, 250 K; △, 350 K; □, 450 K).

density equations and less than 0.05 % relative deviations over the same pressure range for methane and ethane with respect to reference density equations.

3.1. Density. Comparisons against the AGA8 and GERG04 equations were made for all of the experimental density points. For the relative difference of experimental density and the values computed by the AGA-8 and GERG04, the following equations are used:

$$\Delta_{\mathrm{AGA8}} = 100 \cdot \frac{\rho_{\mathrm{exp}} - \rho_{\mathrm{AGA8}}}{\rho_{\mathrm{AGA8}}} \quad (3)$$

$$\Delta_{\mathrm{GERG04}} = 100 \cdot \frac{\rho_{\mathrm{exp}} - \rho_{\mathrm{GERG04}}}{\rho_{\mathrm{GERG04}}} \quad (4)$$

We previously published a detailed analysis of the *force transmission error* for our magnetic suspension densimeter, and the density values reported in Tables 2, 3, and 4 are processed based on the correction correlations in the related literature.[26]

In Table 6 average absolute deviations (AAD) are given for all of the samples. Relative experimental density deviations with respect to AGA8 EOS and GERG04 EOS are given in Figures 1 and 2. The lowest pressure point is 10 MPa, and this might not be low enough for such mixtures to observe the ideal-gas limit as the pressure approaches to zero. Density deviations approach zero below 10 MPa (ideal-gas limit) for the same mixtures, which is shown by McLinden.[2]

For SNG-2 both at low and high pressures, the GERG04 equation shows better performance compared to AGA8.

For SNG-3, GERG04 shows better performance at low pressure up to 40 MPa, and between (40 to 150) MPa, both GERG04 and AGA8 have similar performance in density predictions around the −0.4 % relative deviation band in density. However, for the SNG-3 mixture at higher pressures, GERG04 showed that relative deviations in density have large numbers around −0.6 %, and for the same mixture only at 450 K, AGA had slightly better performance for the pressures beyond 40 MPa.

For SNG-4 sample, the AGA8 equation has better performance than GERG04. However, for the SNG-4 mixture at 350 K measurements and pressures up to 40 MPa, the GERG04 equation has better performance.

3.2. Phase Envelopes. Experimental phase envelopes of the mixtures are plotted in Figure 3. Phase envelopes calculated by various EOS's have significant deviations from the data. The experimental phase envelope data for the mixtures studied in this work appear in Table 3 and Figure 4. For all of the samples, $T/T_{\text{cricondentherm}} < 0.85$, the relative deviation in temperature. $\Delta T/T$ is about constant at 0.1 % or less; however, above 0.85 it grows to about 2 % very near to $T_{\text{cricondentherm}}$. The relative deviation in pressure, $\Delta P/P$, is about 0.025 % for $P/P_{\text{cricondentherm}} < 0.85$ and grows to about 0.23 % as P approaches $P_{\text{cricondentherm}}$.

The uncertainties of the phase envelope measurements are sensitive to changes in composition, especially during when isochores are crossing the phase boundary, and thus the adsorption effect in the isochoric cell shall be minimized during measurements. If possible, this effect shall be monitored accurately by constant sampling from the isochoric cell without disturbing the equilibrium to account by formal uncertainty analysis rather than using the composition information given on the measured gas sample bottles.

Relative percentage deviations of experimental cricondentherm (CT), cricondenbar (CB), and calculated CT and CB values calculated via biparametric cubic, triparametric cubic, and molecular-based EOS's are reported for all of the samples. These values are given for the best-performing EOS in Table 7, which were calculated by the following equation:

$$\Delta_{\text{CT}} = 100 \cdot \frac{\text{CT}_{\text{exp}} - \text{CT}_{\text{EOS}}}{\text{CT}_{\text{EOS}}} \tag{5}$$

$$\Delta_{\text{CB}} = 100 \cdot \frac{\text{CB}_{\text{exp}} - \text{CB}_{\text{EOS}}}{\text{CB}_{\text{EOS}}} \tag{6}$$

For SNG-3 SRK, TRK, and SAFT showed better performance among the equations used. For the SNG-2 and SNG-3 mixtures, the above equations showed better performance in the CT region as shown in Figures 5 and 6 in comparison with CB regions. For SNG-4, the cubic equations were not as successful as molecular-based equations in predicting either the CT or the CB regions of the phase envelope of the mixture, as shown in Figure 7. Among the molecular-based equations, SAFT gave reasonable predictions in the CT regions; however, the CB region predictions from SAFT equation were not close to the experimental values, and there was a huge prediction failure for this mixture in the CB region.

3.3. Uncertainties. All uncertainties for density measurements were reported are standard ($k = 1$) uncertainties, corresponding to a 68 % confidence interval. For sample uncertainties, the supplier did not provide an uncertainty statement for the composition, and McLinden estimated this as 0.00005 mass fraction for each component. The mixture compositions are given in Table 1.

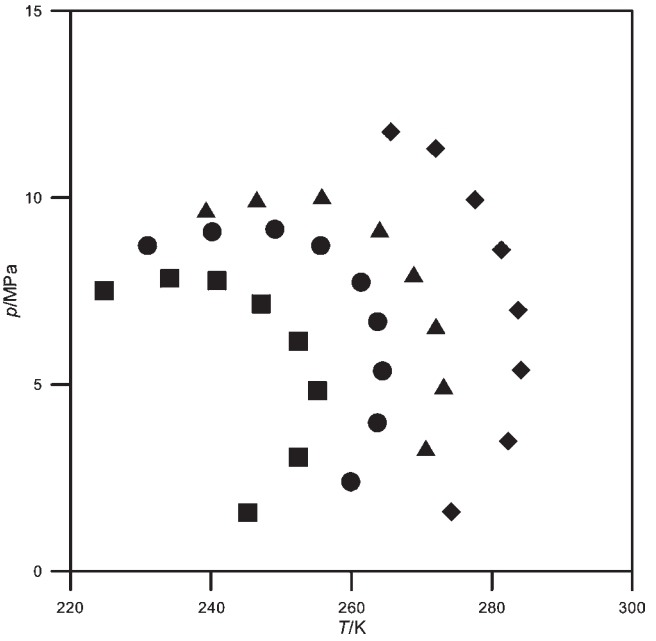

Figure 3. Comparison among measured isochores for SNG-1[1] and SNG-2,3,4 samples. Symbols: ●, SNG1; ■, SNG2; ▲, SNG3; and ◆, SNG4.

The densimeter has an uncertainty specification from the manufacturer of 0.005 $\text{kg}\cdot\text{m}^{-3}$ for densities in the range (0 to 2000) $\text{kg}\cdot\text{m}^{-3}$ over a temperature range of (193.15 to 523.15) K and a pressure range (up to 200) MPa with a maximum pressure of 130 MPa at 523.15 K. The sinker used for measurements in this work was a titanium cylinder having a volume of 6.74083 ± 0.0034 cm^3 with ($k = 1$) an uncertainty of ± 0.05 % in volume and a mass of 30.39157 g, both measured at $T = 293.15$ K and $P = 1$ bar by the manufacturer. Temperature control utilized a PID algorithm implemented in LabVIEW8.0, and the temperature measurements have an uncertainty of 5 mK (including reference resistor and triple point of water cell that is used for temperature sensor calibraion) and average stability of 5.7 mK. A coupling and decoupling device couples the sinker magnetically to a commercial analytical balance (Mettler AT 261) with a measuring range of (0 to 62) g with an uncertainty of 0.03 mg in weighing.

The total uncertainty of the measurements comes from the uncertainties in pressure and temperature measurements and compositions. The error in density caused by pressure, temperature, and composition is:

$$\Delta\rho = \left\{ \Delta\rho^2 + \left[\left(\frac{\partial\rho}{\partial P} \right)_{T,x} \Delta P \right]^2 + \left[\left(\frac{\partial\rho}{\partial T} \right)_{P,x} \Delta T \right]^2 + \left[\left(\frac{\partial\rho}{\partial x_i} \right)_{T,x} \Delta x_i \right]^2 \right\}^{1/2} \tag{7}$$

Uncertainties caused by mixture impurities, temperature, and pressure measurements of the measurements are calculated

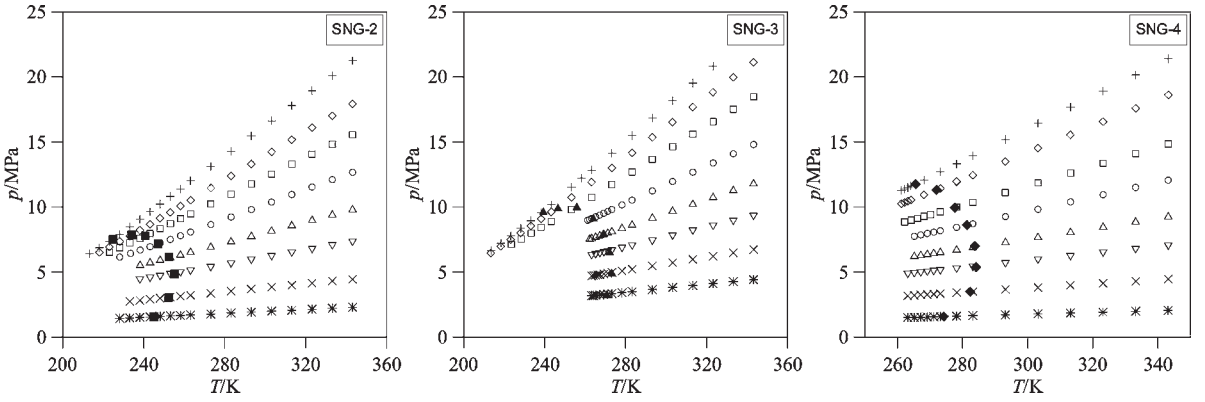

Figure 4. Phase envelopes and experimental isochores for ■, SNG-2; ▲, SNG-3; and ◆, SNG-4.

Table 7. Relative Percentage Deviations on CT and CB Values from Experimental Values and EOS Predictions

sample	biparametric EOS	ΔCT	ΔCB	triparametric EOS	ΔCT	ΔCB	molecular EOS	ΔCT	ΔCB
SNG-2	PR	−0.754	−6.23	PT	−0.616	−4.506	PC-SAFT	−0.875	−0.595
SNG-3	SRK	0.0216	5.033	TRK	0.458	3.335	SAFT	−0.247	−2.901
SNG-4	SRK	2.15	19.49	MMM	2.76	22.06	SAFT	1.05	9.39

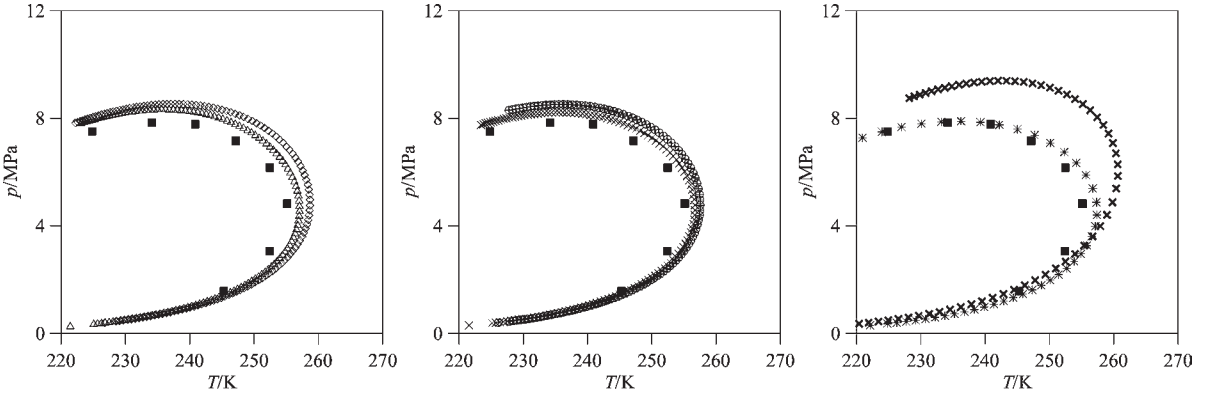

Figure 5. Experimental phase envelope for ■, SNG-2 and calculated phase envelopes (a) from △, PR EOS; ◇, SRK EOS; (b) from ×, PT EOS and ○, MMM EOS; (c) from ×, SAFT EOS and ∗, PC-SAFT EOS.

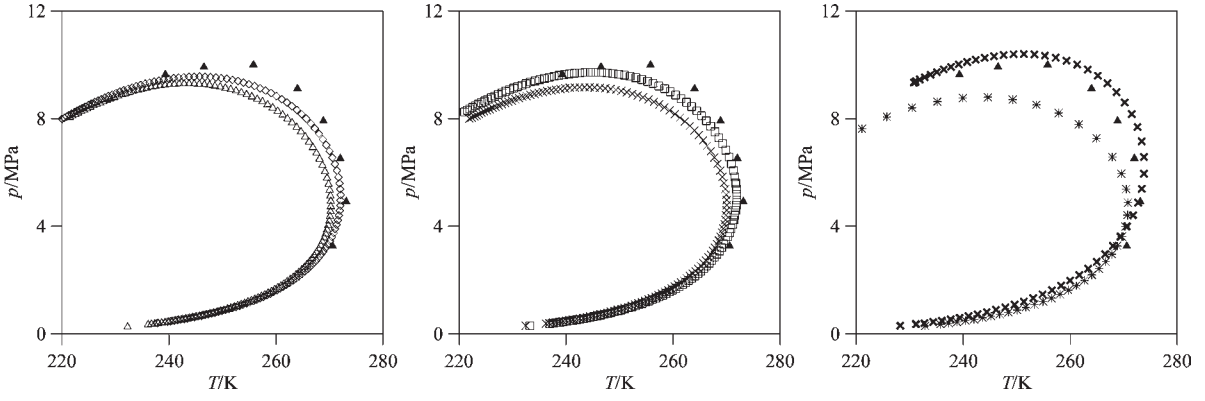

Figure 6. Experimental phase envelope for ▲, SNG-3 and calculated phase envelopes (a) from △, PR EOS; ◇, SRK EOS; (b) from ×, PT EOS and □, TRK EOS; (c) from ×, SAFT EOS and ∗, PC-SAFT EOS.

with an uncertainty of 0.13 % ($k = 1$) in density. The temperature and pressure uncertainties are only a small contribution to the overall uncertainty. The biggest contribution to the overall uncertainty comes from the mixture uncertainties. For each component,

dx.doi.org/10.1021/je200438t |J. Chem. Eng. Data 2011, 56, 3766–3774

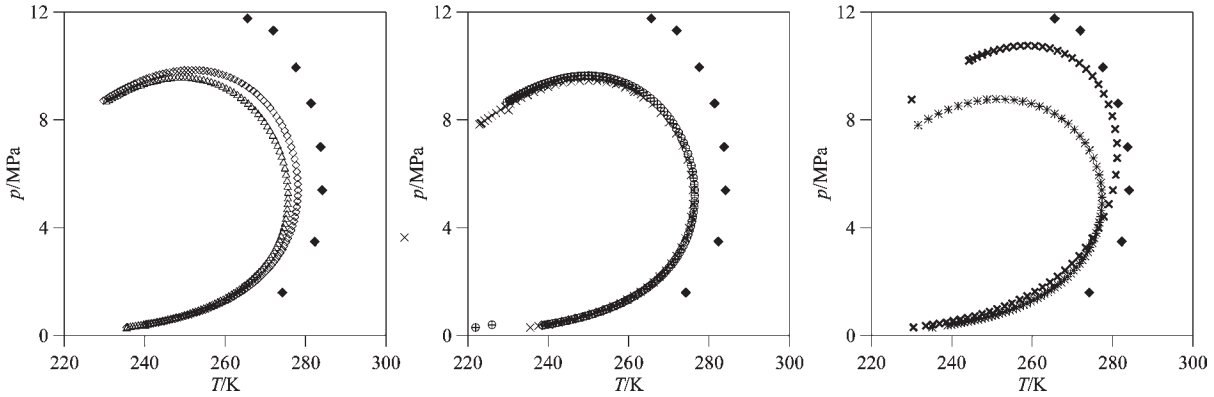

Figure 7. Experimental phase envelope for ◆, SNG-4 and calculated phase envelopes (a) from △, PR EOS; ◇, SRK EOS; (b) from ×, PT EOS and ○, MMM EOS; (c) from ×, SAFT EOS and ∗, PC-SAFT EOS.

an uncertainty of 0.00005 in mass fraction is assumed.[2] This yields to the relative uncertainty in density for a given mixture around 0.008 % to 0.009 % (k = 1). Thus, the total effect of the mixture uncertainty in density is calculated as 0.025 % (k = 1); when this value is compared with the combined uncertainties that come from the temperature and pressure measurements as calculated as (k = 1) 0.01 %, it is clearly seen that the uncertainties that come from mixture compositions have a larger effect on the overall uncertainties of the measurements.

For the isochoric apparatus, the temperature stability of the measurements within the cell was ± 5 mK measured via a platinum resistance thermometer. A quartz pressure transducer from Paroscientific Inc. measures pressure within the cell with a manufacturer specified relative uncertainty of ± 0.01 % of full scale or 0.0035 MPa for the 35 MPa transducer used for in this apparatus. The transducer temperature is held constant at 343.15 K during the measurements, well above the mixture cricondentherm. Mixture uncertainties for isochoric measurements are the same as calculated for mixture uncertainties for densimeter measurements, since the same mixtures are used in both measurements.

Due to pressure and temperature variations of the isochoric cell, the volume of the cell changes; thus, these variations are corrected by using the isothermal compressibility and volume expansivity coefficients of the stainless steel cell.

4. CONCLUSION

We measured the density and the phase envelopes of three synthetic natural gas mixtures with varying compositions. The experimental density results were compared to the GERG04 and the AGA8 equations as they are the two leading industrial equations for natural gas density calculations. GERG04 shows a little better predicting performance when compared with AGA8 within the proposed predicting ranges for both EOS. Yet, the performance of GERG04 is better, especially for the pressure up to 40 MPa, which is the more realistic condition case for pipeline custody transfer.

For phase envelopes, for the SNG-2 and SNG-3 mixtures, bi- and triparametric cubic equations and molecular-based equations have shown better performance in predicting the CT regions, and yet, all of these equations have shown some deviations in the CB regions. For the SNG-4 mixture, except for the PC-SAFT equation, none of the equations were able to show agreement with the CT region. Moreover, for the SNG-4 mixture, neither PC-SAFT nor any other molecular-based equation could predict the CB region accurately. We believe that the reasons in CT and CB region calculations via equations are due to the higher fractions of propane and the butanes since carbon dioxide and nitrogen are removed in the SNG-4 mixture.

■ ASSOCIATED CONTENT

Supporting Information. Ischoric results for SNG-2, SNG-3, and SNG-4 (Tables S1, S2, and S3) and SNG-2, SNG-3, and SNG-4 mixture density deviation comparisons between this work and NIST (Figures S1, S2, and S3). This material is available free of charge via the Internet at http://pubs.acs.org.

■ AUTHOR INFORMATION

Corresponding Author

*E-mail: mert.atilhan@qu.edu.qa.

Funding Sources

The authors also acknowledge the Texas Engineering Experiment Station (TEES) and Qatar National Research Funds (QNRF Project No. NPRP-30-6-7-1) for financial support. S. A. additionally acknowledges the USA-Spain Fulbright Commission and Ministerio de Educación y Ciencia (Spain).

■ ACKNOWLEDGMENT

Authors would like to thank Mark McLinden from NIST for technical discussion and collaboration.

■ REFERENCES

(1) Atilhan, M.; Aparicio, S.; Ejaz, S.; Cristancho, D.; Hall, K. R. $P-\rho-T$ Behavior of a Lean Synthetic Natural Gas Mixture Using Magnetic Suspension Densimeters and an Isochoric Apparatus: Part I. *J. Chem. Eng. Data* **2011**, *56* (2), 212–221.

(2) McLinden, M. O. $p-\rho-T$ Behavior of Four Lean Synthetic Natural-Gas-Like Mixtures from 250 to 450 K with Pressures to 37 MPa. *J. Chem. Eng. Data* **2011**, *56* (3), 606–613.

(3) Atilhan, M. A New Cubic Equation of State, Master Thesis. Texas A&M University, College Station, TX, 2004.

(4) Danesh, A. *PVT and phase behaviour of petroleum reservoir fluids*; Elsevier: Amsterdam, 1998.

(5) Nasrifar, K.; Bolland, O. Predicting Natural Gas Dew Points from 15 Equations of State. *Energy Fuels* **2005**, *19*, 561–572.

(6) Jarne, C.; Avila, S.; Blanco, S. T.; Rauzy, E.; Otin, S.; Velasco, I. Thermodynamic Properties of Synthetic Natural Gases. 5. Dew Point Curves of Synthetic Natural Gases and Their Mixtures with Water and with Water and Methanol: Measurement and Correlation. *Ind. Eng. Chem. Res.* **2003**, *43* (1), 209–217.

(7) Zhou, J. J.; Patil, P.; Ejaz, S.; Atilhan, M.; Holste, J. C.; Hall, K. R. (p, V-m, T) and phase equilibrium measurements for a natural gas-like mixture using an automated isochoric apparatus. *J. Chem. Thermodyn.* **2006**, *38* (11), 1489–1494.

(8) Starling, K. E.; Luongo, J. F.; Hubbard, R. A.; Lilly, L. L. Inconsistencies in dew points from different algorithm types possible causes and solutions. *Fluid Phase Equilib.* **2001**, *183*−*184*, 209–216.

(9) Kunz, O.; Klimeck, R.; Wagner, W.; Jaeschke, M. *The GERG-2004 Wide-Range Equation of State for Natural Gases and Other Mixtures*; GERG TM15; Fortschritt-Berichte VDI: Weinheim, Germany, 2007.

(10) Starling, K. E.; Savidge, J. L. *Compressibility Factors of Natural Gas and Other Related Hydrocarbon Gases*; American Gas Association: Arlington, VA, 1992.

(11) Peng, D.-Y.; Robinson, D. B. A New Two-Constant Equation of State. *Ind. Eng. Chem. Fundam.* **1976**, *15* (1), 59–64.

(12) Soave, G. Equilibrium constants from a modified Redlich-Kwong equation of state. *Chem. Eng. Sci.* **1972**, *27* (6), 1197–1203.

(13) Twu, C. H.; Coon, J. E.; Cunningham, J. R. A new generalized alpha function for a cubic equation of state Part 2. Redlich-Kwong equation. *Fluid Phase Equilib.* **1995**, *105* (1), 61–69.

(14) Patel, N. C.; Teja, A. S. A new cubic equation of state for fluids and fluid mixtures. *Chem. Eng. Sci.* **1982**, *37* (3), 463–473.

(15) Mohsen-Nia, M.; Modarress, H.; Mansoori, G. A. A cubic hard-core equation of state. *Fluid Phase Equilib.* **2003**, *206* (1−2), 27–39.

(16) Muller, E. A.; Gubbins, K. E. Molecular-Based Equations of State for Associating Fluids: A Review of SAFT and Related Approaches. *Ind. Eng. Chem. Res.* **2001**, *40* (10), 2193–2211.

(17) Tumakaka, F.; Gross, J.; Sadowski, G. Thermodynamic modeling of complex systems using PC-SAFT. *Fluid Phase Equilib.* **2005**, *228*−*229*, 89–98.

(18) Atilhan, M.; Ejaz, S.; Zhou, J.; Cristancho, D.; Mantilla, I.; Holste, J.; Hall, K. R. Characterization of Deepwater Natural Gas Samples. Part 1: 78% Methane Mixture with Heavy Components. *J. Chem. Eng. Data* **2010**, *55* (11), 4907–4911.

(19) Wagner, W.; Kleinrahm, R. Densimeters for very accurate density measurements of fluids over large ranges of temperature, pressure, and density. *Metrologia* **2004**, *41* (2), S24–S39.

(20) Doiron, T.; Behringer, R. P.; Meyer, H. Equation of state of He3/He4 mixture near its liquid-vapor critical point. *J. Low Temp. Phys.* **1976**, *24* (3), 345–363.

(21) Acosta-Perez, P. L.; Cristancho, D. E.; Mantilla, I. D.; Hall, K. R.; Iglesias-Silva, G. A. Method and uncertainties to determine phase boundaries from isochoric data. *Fluid Phase Equilib.* **2009**, *283* (1−2), 17–21.

(22) Cristancho, D. E.; Mantilla, I. D.; Ejaz, S.; Hall, K. R.; Atilhan, M.; Iglesia-Silva, G. A. Accurate *P*-*ρ*-*T* Data for Methane from (300 to 450) K up to 180 MPa. *J. Chem. Eng. Data* **2009**, *55* (2), 826–829.

(23) Cristancho, D. E.; Mantilla, I. D.; Ejaz, S.; Hall, K. R.; Atilhan, M.; Iglesias-Silva, G. A. Accurate *P*-*ρ*-*T* Data for Ethane from (298 to 450) K up to 200 MPa. *J. Chem. Eng. Data* **2010**, *55* (8), 2746–2749.

(24) Mantilla, I. D.; Cristancho, D. E.; Ejaz, S.; Hall, K. R.; Atilhan, M.; Iglesias-Silva, G. A. New *P*-*ρ*-*T* Data for Nitrogen at Temperatures from (265 to 400) K at Pressures up to 150 MPa. *J. Chem. Eng. Data* **2010**, *55* (10), 4227–4230.

(25) Mantilla, I. D.; Cristancho, D. E.; Ejaz, S.; Hall, K. R.; Atilhan, M.; Iglesias-Silva, G. A. *P*-*ρ*-*T* Data for Carbon Dioxide from (310 to 450) K up to 160 MPa. *J. Chem. Eng. Data* **2010**, *55* (11), 4611–4613.

(26) Cristancho, D.; Mantilla, I.; Ejaz, S.; Hall, K.; Iglesias-Silva, G.; Atilhan, M. Force Transmission Error Analysis for a High-Pressure Single-Sinker Magnetic Suspension Densimeter. *Int. J. Thermophys.* **2010**, *31* (4), 698–709.